23rd ABCM International Congress of Mechanical Engineering
December 6-11, 2015, Rio de Janeiro, RJ, Brazil

ANALYSIS OF WRENCH CAPABILITY FOR COOPERATIVE ROBOTIC SYSTEMS.

Julio Cesar Frantz
Leonardo Mejia Rincon
Henrique Simas
Daniel Martins
Federal University of Santa Catarina, 88040-900 Florianópolis, SC, Brazil
julio.frantz@posgrad.ufsc.br
leonardo.mejia.rincon@posgrad.ufsc.br
henrique.simas@ufsc.br
daniel.martins@ufsc.br

Abstract. *Recently, industrial robots are being more and more widely used in a variety of machining applications, such as drilling, milling and grinding because of their flexibility in performing tasks in a relatively small space, and furthermore, at a lower cost. In many cases, the wrench capability of industrial robots is lower than the required, causing in some tasks the saturation of the joints. The possibility of using two or more robots to perform a given task increases the wrench capability, allowing us to workout in applications which are impossible to solve by using only one manipulator. A Cooperative Robotic System (CRS) increases the flexibility in the performance of tasks allowing a more homogeneous distribution of the forces generated during the interaction between the end-effector and the environment. In some cases, the CRS can be composed by robots with different capabilities, and a strategy for wrench distribution must be used. Recent works presented the force capability analysis using an scaling factor method for single serial robots. This paper proposes the use of this scaling factor method in CRS, seeking to obtain a balance of forces between the robots. The proposed method is discussed and graphical results are presented.*

Keywords: *Robotics, force capability, screw theory, Davie's method.*

1. INTRODUCTION

Machine tools are increasingly being required in industry due to the need for adaptability, productivity and quality in manufacturing process that are extremely important. In this scenario are included the industrial robots.

According to Subrin *et al.* (2011) compared with a 5-axes machine tool, robots have a higher workspace and lower investment, but have limitations in power applications such as the case of the machining process. The major fields of cutting applications for industrial robots are prototyping, cleaning and pre-machining of middle tolerance parts (Abele *et al.*, 2007).

When a robot is used to perform a machining application the excessive forces between the tool and the workpiece cause deformations in the links of the kinematic chain, affecting the accuracy of the workpiece (Pan *et al.*, 2006; Coelho *et al.*, 2011). These deformations will be absorbed by the robot structure, but due to the design of the serial chain and the low torsional stiffness of the actuators, the accuracy and the quality of the process are affected (Owen *et al.*, 2008).

The basic requirement for applying a robot machining operation is the control of the interaction forces with the environment (Alici, 1999). The interaction forces can be measured by a force/torque sensor attached to the end effector of the manipulator. But to study the behaviour of forces during machining operations, like milling and drilling, the forces/torques can also be calculated through mathematical models (Cruz, 2010).

The main goal of this work is to solve the wrench capability of Cooperative Robotic Systems (CRS) applying the scaling factor method presented by Nokleby *et al.* (2005) and to solve the wrench distribution for CRS using the scaling factor method. A CRS is a system composed by several robots that help each other or collaborate in the accomplishment of one or more tasks simultaneously. Due to the flexibility of using two or more robots, it's possible to perform complex tasks and tasks that require greater load capacity or heavier-weight collaborative processes, for example: packaging, palletizing, assembly and machining. Knowing the force capability of the CRS, it's possible to evaluate some machining applications, like prototyping.

Some studies related to the wrench distribution in CRS can be found in the literature, however the solution to this kind of problem using the scaling factor method it's not found. The problem of wrench distribution in parallel mechanism are presented in different literature (Zheng and Luh, 1988; Kumar and Waldron, 1988; Walker *et al.*, 1989).

When a CRS share the load, the total number of degrees of freedom is usually greater than the workspace, so it's possible to use the actuator redundancy to optimize certain kinds of performance, like the wrench distribution (Zheng and Luh, 1988).

Hsu (1993) discuss the problem of used two robots to sustain a common load. If the wrench distribution strategy fail, any of the robot can overload. Caccavale and Uchiyama (2008) presented the static solution for a CRS using the Jacobian, and used a conceptual approach called *virtual sticks* to connect the end-effectors to the main frame fixed in the workpiece.

The force capability of a robotic mechanism is defined as the maximum wrench that can be applied (or sustained) for a given pose, based on the limits of its actuators (Nokleby *et al.*, 2005). Force capability studies are presented in Papadopoulos and Gonthier (1995) and Nokleby *et al.* (2005), in these studies the scaling factor method is used to generate a force capability polygon for the given pose. The force capability of a robot is dependent on its design, posture, actuation limits and redundancies (Weihmann *et al.*, 2011).

Several studies related to the force capability and the force distribution in single manipulators can be found in the literature. Zibil *et al.* (2007) presented the scaling factor method and the explicit method to evaluate the force capabilities of parallel manipulators. Firmani *et al.* (2008) developed the force capability polygon using the maximum force with a prescribed moment (F_{app}). If the prescribed moment is zero, it yields a pure force analysis and the maximum force that can be applied (or sustained) will be denoted as F_m.

Recent works guided by Weihmann *et al.* (2011) and Mejia *et al.* (2014) used differential evolution algorithms (DE) to evaluate the force capability of planar parallel manipulators. Mejia *et al.* (2015) developed a mathematical closed-form solution to obtain the force capability polytope of mechanism with 3 degrees of freedom. In this methodology Mejia *et al.* (2015) used screw theory and Davies method as primary mathematical tools to solve the kinematic and static of the mechanisms.

The remainder of this work is structured as follows: In Section 2 the forces acting in a twist drill during a drilling operation are described. Section 3 provides a description of the case under study. Section 4 explains the scaling factor method. Simulation results are presented and discussed in Section 5. Finally, Section 6 outlines a brief conclusion about this study.

2. FORCE ANALYSIS OF A DRILLING PROCESS

In a drilling process the machining force F_T acting on the drill can be decomposed in components such as the cutting force f_c, feed force f_f, passive force f_p and the reaction torque m_z as shown in Fig.1.

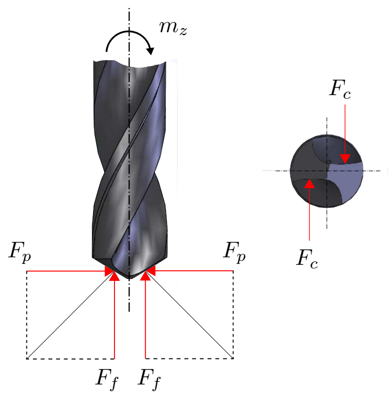

Figure 1: Forces acting on a twist drill.

The empirical Kienzle model describes the behaviour of the machining forces and adopts a potential function, especially with a view to practical applications, developed for the turning process in general Eq. (1) (Stemmer, 1989).

$$F_c = k_{c1.1} \cdot b \cdot h^{1-m_c} \tag{1}$$

where:

$k_{c1.1}$ - specific cutting force to *b* x *h* = 1 mm^2;

b - chip width;

h - chip thickness;

1-m_c - Kienzle exponent.

Based on the Kienzle model, Witte (1980) *apud* (Boeira *et al.*, 2009) developed equations for determining the force components and reaction torque in drilling process, Eqs. (2), (3) and (4).

$$f_c = k_c \cdot \frac{f \cdot d}{4} \tag{2}$$

$$f_f = k_f \cdot \frac{f \cdot d \cdot \sin(\frac{\sigma}{2})}{2} \tag{3}$$

$$m_z = k_c \cdot \frac{f \cdot d^2}{8000} \tag{4}$$

where:

k_c - specific cutting force;

k_f - specific cutting feed;

f - feed;

d - drill diameter;

σ - tool tip angle.

To determine the components of the machining force it's necessary to know the force and feed cutting constant and the cutting parameters. The values of the constants are determined from experimental tests, and for a wide range of materials these values have already been determined. A table with the values of $1 - m_c$ and $k_{c1.1}$ for some types of materials can be found in Stemmer (1989).

In Table 1 can be visualized the feed force, reaction torques and power values required for machining some materials. The results are obtained using a twist drill of 2 mm diameter, feedrate (f) of the drilling operation 0.2 mm, cutting speed (v_c) of 30 m/min, tilt drill angle $4°$ and clearance angle $12°$.

Table 1: Machining forces during a drilling operation.

Material	k_c (N/mm^2)	f_f (N)	m_z (Nm)	P (kW)
Steel carbon ABNT 1020	2862	83	0.3	0.14
Al 2024	1724	50	0.2	0.09

Through the machining forces obtained in Tab. 1, it's possible to evaluate the wrench capability of a robot when applied for a drilling operation.

3. STATICS OF COOPERATIVE ROBOTIC SYSTEMS

In the statics analysis of CRS, the main goal is to determine the force and moment requirements for the joints in relation to the wrenches applied at the end-effector. In this work the formalism presented by Davies (Davies, 2006) is used as the mathematical tool to analyse the static problem. The Davies method appears in many publications in the literature and further explanations can be found in (Davies, 2006; Weihmann *et al.*, 2011; Mejia *et al.*, 2015).

The Davies method establishes a systematic way to relate the forces and moments in closed kinematic chains (Weihmann *et al.*, 2011). This method is based in graph theory, screw theory and Kirchhoff-Davies cut-set law and circuit law and it can be used to obtain the static equations of a robot in a matricial form (Weihmann *et al.*, 2011).

The CRS under study is composed for two 3R planar robots, one called *Leader* (with the tool fixed at the end-effector) and another called *Follower* (with the workpiece fixed at the end-effector) as shown in Fig. 2a. Using screw theory the wrenches (force and moments) applied by the end-effector can be represented by the vector $\$_F = [f_x\, f_y\, m_z]^T$ where f_x and f_y denotes the force in the directions x and y respectively, and m_z denotes the moment around the z axis. The torques at the actuated joints in the leader and the follower manipulators are denoted as τ_a, τ_b, τ_c and τ_d, τ_e, τ_f as shown in Fig. 2a.

Using graph theory and the cut-set law (Davies, 2006), it is possible to prove that the gross of this manipulator is C=24 and, in the absence of singularities, the nett degree of constraint is $C_N = 3$. The nett degree of constraint $C_N = 3$ means that only three independent variables are needed in order to solve the statics of the CRS. The CRS action graph is

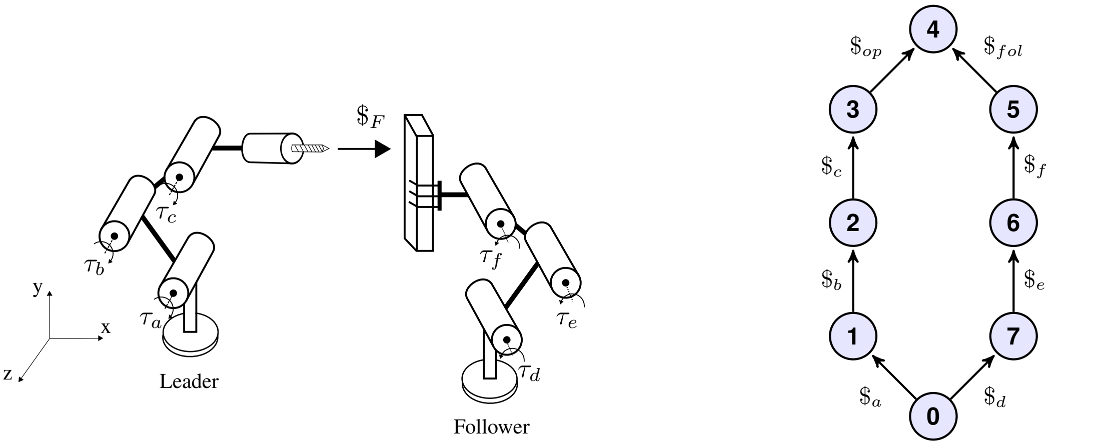

(a) Planar CRS.

(b) Action graph of the planar CRS.

Figure 2: Planar CRs and the respectively action graph.

shown in Fig. 2b, where the edges are the joints and the vertex are the manipulator links. The wrenches in each joint are represented by the symbol \$.

Considering the primary variables as the wrenches acting in the end-effector, the static solution can be written in the form:

$$\{\Psi_s\}_{21\times 1} = \left[-\hat{A}_{N_s}^{-1}\right]_{21\times 21} \left[\hat{A}_{N_p}\right]_{21\times 3} \begin{Bmatrix} f_x \\ f_y \\ m_z \end{Bmatrix} \tag{5}$$

where Ψ_s is the secondary variables magnitudes, $\hat{A}_{N_s}$ is the unitary action matrix of the secondary variables and $\hat{A}_{N_p}$ is the unitary action matrix of the primary variables, where all wrenches must be written in the same reference frame.

Equation (5) can be rewritten in its unfolded form as shown in Eq. (6). In this new representation, it's possible to select the secondary variables in the vector Ψ_s, selecting the torques in the actuated joints. Multiplying the primary and secondary matrix it's possible to extract the eighteen kinematic variables $a_1, \ldots, a_{18}$ (where the $a_1, \ldots, a_{18}$ terms represent kinematic expressions as a function of the manipulator joint positions (Frantz, 2015)).

$$\begin{Bmatrix} \tau_a \\ \tau_b \\ \tau_c \\ \tau_d \\ \tau_e \\ \tau_f \end{Bmatrix} = \begin{bmatrix} a_1 & a_2 & a_3 \\ a_4 & a_5 & a_6 \\ a_7 & a_8 & a_9 \\ a_{10} & a_{11} & a_{12} \\ a_{13} & a_{14} & a_{15} \\ a_{16} & a_{17} & a_{18} \end{bmatrix} \begin{Bmatrix} f_x \\ f_y \\ m_z \end{Bmatrix} \tag{6}$$

The solution obtained in Eq. (6) is similar to the classic static mapping obtained through virtual working method (Siciliano *et al.*, 2009). But the solution used in this work is not restricted to the absence of gravity.

4. SCALING FACTOR METHOD

The scaling factor strategy presented by Nokleby *et al.* (2005) consists of applying a unit force in the desired direction and determine the robot joint overloaded (Weihmann *et al.*, 2011). Using this method the actuator limits are easily incorporated into the problem of determining the force-moment capabilities of robotic manipulators (Nokleby *et al.*, 2005).

In the scaling factor method a unit wrench $\$_F$ is used to represent the desired wrench direction as shown in Eq. (7). In this equation f_{app} is the wrench intensity of F_{app}.

$$F_{app} = f_{app}\,\$_F \tag{7}$$

The wrench at the end effector F_{app} of the manipulator can be denoted as $f = [f_x,\, f_y,\, f_z]$ and $m = [m_x,\, m_y,\, m_z]$ respectively. Using the planar case ($\lambda = 3$) as example, it's possible to represent the desired wrench direction in terms of the θ angle, in order to represent the maximum force F_T applied (or sustain) by the end-effector.

Using the unit wrench $\$_F = [\cos(\theta), \sin(\theta), 0]^T$ in order to represent the desired direction of the force, and for a single 3R planar robot, Eq. (6) can be rewritten as shown in Eq. (8) (Frantz, 2015). Note that the prescribed moment is equal to zero (m_z = 0), it yields a pure force analysis (F_m).

$$\begin{Bmatrix} \tau_a \\ \tau_b \\ \tau_c \end{Bmatrix} = \begin{bmatrix} a_1 & a_2 & a_3 \\ a_4 & a_5 & a_6 \\ a_7 & a_8 & a_9 \end{bmatrix} \begin{Bmatrix} \cos(\theta) \\ \sin(\theta) \\ 0 \end{Bmatrix} \tag{8}$$

Expanding Eq. (8), it is possible to know the values of τ_a , τ_b and τ_c as a function of θ. The expansion of Eq. (8) is shown below in Eqs. (9), (10) and (11).

$$\tau_a = a_1 \cos(\theta) + a_2 \sin(\theta) \tag{9}$$

$$\tau_b = a_4 \cos(\theta) + a_5 \sin(\theta) \tag{10}$$

$$\tau_c = a_7 \cos(\theta) + a_8 \sin(\theta) \tag{11}$$

Since all maximum actuated joint torque/force limits $\tau_{i_{max}}$ are known for all actuated joints i, scaling factors for each actuated joint can be found using Eq. (12) (Nokleby *et al.*, 2005). In this equation, sf_i is the scaling factor for each actuated joint i, and τ_i is the torque/force of the i^{th} actuated joint for a unit wrench in the desired force direction, obtained from Eqs. (9), (10) and (11).

$$sf_i = \left| \frac{\tau_{i_{max}}}{\tau_i} \right| \quad i = 1, 2, 3. \tag{12}$$

The scaling factors of Eq. (12) can be placed in a set. The scaling factor (Φ) in this set with the minimum value is the maximum factor which all joint torques/forces can be scaled by and still remain at or below their corresponding maximum values (Nokleby *et al.*, 2005), $i.e.$:

$$\Phi = \min(sf_i) \quad i = 1, 2, 3. \tag{13}$$

The force capability is determined multiplying the scaling factor (Φ) by both sides of the Eq. (8). It is possible to see the effects of the scaling factor in a better way, as shown in Fig. 3.

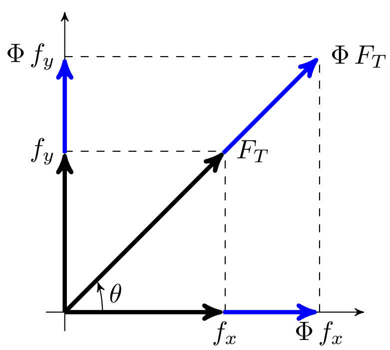

Figure 3: Scale factor applied to the wrench at the end-effector of the manipulator.

In Figure 3, notice that the use of the scale factor implies that the force F_T at the end-effector will be scaled for a Φ value. In practice, the scale factor will allow the robots' actuators (in a particular posture) achieve the limits of saturation, without suffering any damage.

Using the scaling factor method it's possible to obtain the force capability polygon and the maximum joint torque map. The force capability polygon represents the maximum force that the end-effector of the robot can apply or sustain in the *x* and *y* directions of the base frame, with the prescribed moment $m_z = 0$ and $\theta \in [0, 2\pi]$.

5. APPLICATIONS AND RESULTS

The results of apply the scaling factor method in a Cooperative Robotic System (CRS) is discussed in this section. The schematic representation of the studied CRS is shown in Fig. 2a, this is a planar CRS with mobility equal to six (M = 6) and with a nett degree of restriction equal to three ($C_N = 3$). The static of the CRS was solved using the formalism presented by Davies (2006) as was previously discussed in Section 3 and the particular backward statics solution for the CRS looks like shown in Eq. (6).

The graphical results, were obtained using arbitrary topological information for the links: l_1=0.40 m, l_2=0.35 m, l_3=0.25 m, l_4=0.70 m, l_5=0.40 m, l_6=0.25 m, the end effector position (in meters) of the leader robot (x,y) = (-0.15;0.35) and the follower robot (-0.10;0.45), the joint angles (in rad) $(\theta_1, \theta_2, \theta_3, \theta_4, \theta_5, \theta_6) = (\pi, -\pi/2, -\pi/2, \pi/2, \pi/2, \pi/2)$ and the maximum torques in the joints of the leader $\tau_{a_{max}} = \tau_{b_{max}} = \tau_{c_{max}} = \pm$5Nm and the follower $\tau_{c_{max}} = \tau_{d_{max}} = \tau_{e_{max}} = \pm$10Nm.

As was previously discussed in Section 4 the maximum force at the manipulator end-effector is a function of the direction of the force (θ) and the prescribed moment (m_z). In order to obtain our graphical results, the scaling factor method was used with a prescribed moment m_z= 0 [Nm] and with the θ angle $\in [0, 2\pi]$. It allows us to obtain a force capability polygon for the CRS, as shown in Fig. 4. In Fig. 4 the solid blue line represents the force capability polygon of the leader manipulator, and the dashed red line represents the force capability polygon of the follower manipulator.

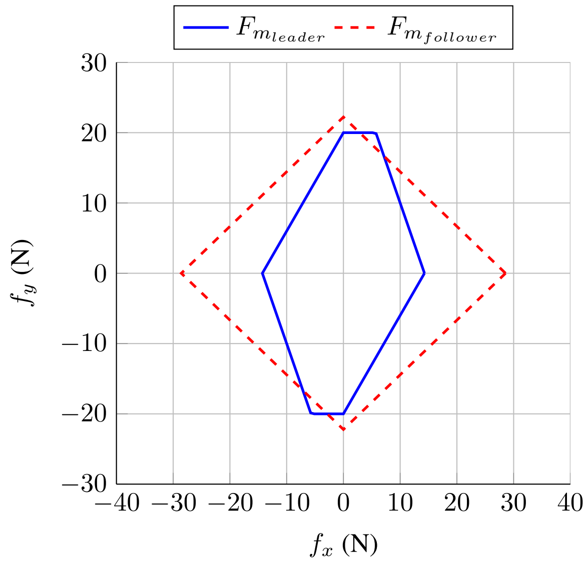

Figure 4: Force capability polygon of the leader and the follower.

Similarly it's possible to obtain the torque capability map, to the leader and follower manipulators respectively, as shown in Figs. 5a and 5b. In these maps, it's possible see that the actuated joints do not exceed the limit of saturation (τ_{max}) in any direction of the applied wrench.

Note that in Fig. 4 the leader and the follower force capability polygon have a different wrench capacities. To found an equilibrium between the robots it's necessary to apply an strategy for the wrench distribution.

The wrench distribution between the leader and the follower manipulators are achieved analysing the force applied or

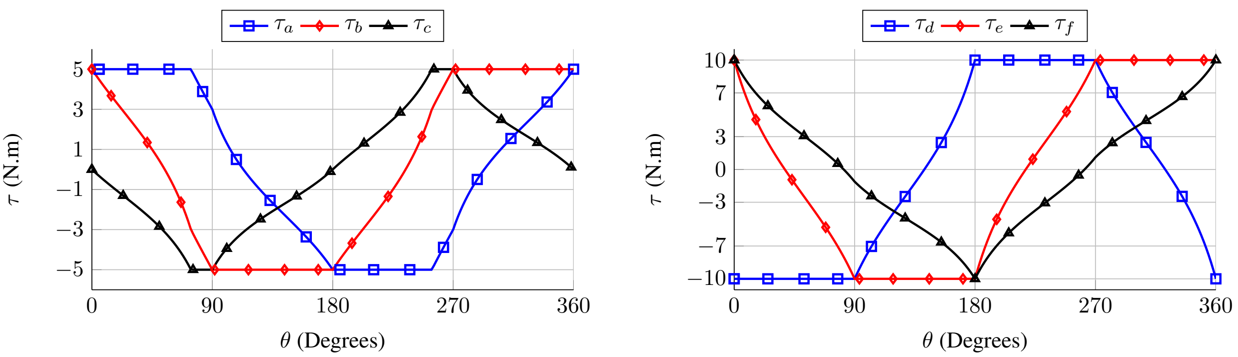

(a) Torque capability map for the leader. (b) Torque capability map for the follower.

Figure 5: Torque capability map for the leader and the follower manipulators.

sustained by the end-effector of the robots. Analysing the force it's possible to find the intersection between the two force capability polygons. The results of apply the wrench distribution strategy is shown in Fig. 6.

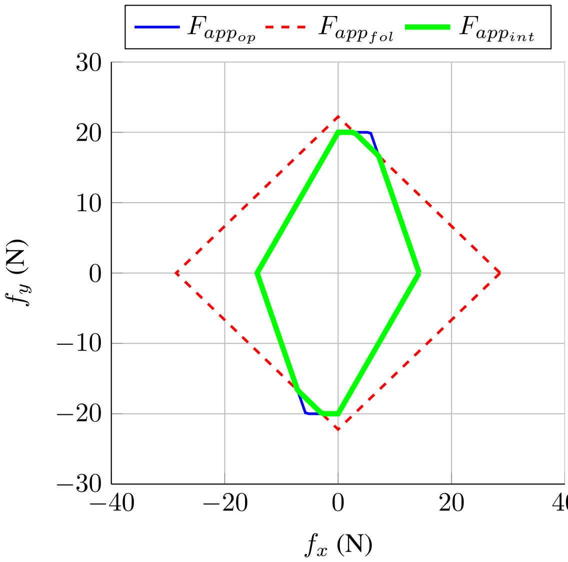

Figure 6: Force capability polygon for the CRS.

In Fig. 6 the solid green line is the intersection between the leader and the follower force capability polygons, determined by the wrench distribution strategy. This strategy makes the force of the robot with greater capacity in the desired position decreases, reducing the force in each actuated joint as shown in Figs. 7a and 7b. In Fig. 7b the dashed lines are the joint torques before applying the strategy, and the solid lines after applying the strategy.

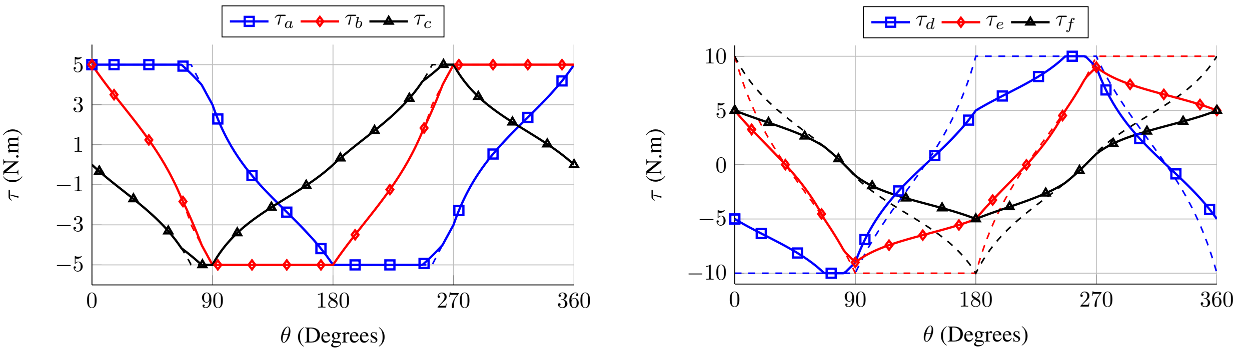

(a) Torque capability map for the leader.

(b) Torque capability map for the follower.

Figure 7: Torque capability map for the leader and the follower manipulators after the wrench distribution strategy.

6. CONCLUSIONS

This work presents a new solution to the determination of the force capability and load distribution of planar Cooperative Robotic Systems. The scale factor and the Davies method were fully addressed to solve the force capability and the static of CRS's.

To illustrate the method, results for a planar CRS were presented. Using the two methods, it is possible to obtain the force and torque capability of a CRS for each position within the CRS's workspace. The presented work may be extended in several ways, allowing its use in spatial CRS or planar CRS with different degrees of freedom.

Evaluating only the force capability of the CRS, excluding the dynamic interactions and position accuracy, the CRS demonstrate force capability to perform drilling tasks. Another works, may consider the mass of the links, the gravity and the gear reducers in order to reproduce the results as closed as possible to practical solutions.

7. ACKNOWLEDGEMENTS

The authors would like to thanks CAPES for the partial financial support.

8. REFERENCES

Abele, E., Weigold, M. and Rothenbücher, S., 2007. "Modeling and identification of an industrial robot for machining applications". *{CIRP} Annals - Manufacturing Technology*, Vol. 56, No. 1, pp. 387 – 390.

Alici, G., 1999. "A systematic approach to develop system for robotic drilling". *Industrial robot: An International Journal*, pp. 389–397.

Boeira, A.M.G., Kuster, F., Wegener, K., Knoblauch, R., Margot, R. and Schroeter, R.B., 2009. "Contribuições a modelagem de forças na furação com brocas helicoidas". *Congresso Brasileiro de Engenharia de Fabricação, BH, MG, Brasil*.

Caccavale, F. and Uchiyama, M., 2008. "Cooperative manipulators". Springer Berlin Heidelberg, Springer Handbook of Robotics, pp. 701–718.

Coelho, R.T., Rodella, H.H.T., Martins, V.F. and Barba, R., 2011. "An investigation into the use of industrial robots for machining soft and low density materials with hsm technique". *J. Braz. Soc. Mech. Sci. & Eng., vol.33 no.3*, pp. 343–350.

Cruz, F.B.C., 2010. *Modelagem, controle e emprego de robôs em processos de usinagem*. Ph.D. thesis, Universidade Federal de Santa Catarina, Florianópolis, Brasil.

Davies, T.H., 2006. "Freedom and constraint in coupling networks". *Proceedings of the Institution of Mechanical Engineers, Part C: Journal of Mechanical Engineering Science*, Vol. 220, No. 7, pp. 989–1010.

Firmani, F., Zibil, A., Nokleby, S. and Podhorodeski, R., 2008. "Wrench capabilities of planar parallel manipulators. part i: Wrench polytopes and performance indices". *Robotica*, Vol. 26, No. 6, pp. 791–802.

Frantz, J., 2015. *Análise estática de sistemas robóticos cooperativos*. Master's thesis, Universidade Federal de Santa Catarina, Florianópolis, Brasil.

Hsu, P., 1993. "Coordinated control of multiple manipulator systems". *IEEE Transactions on Robotics and Automation*, Vol. 9, pp. 400–410.

Kumar, V. and Waldron, K.J., 1988. "Force distribution in closed kinematic chains". *IEEE Journal of Robotics and Automation*, Vol. 4, pp. 657–664.

Mejia, L., Simas, H. and Martins, D., 2014. "Force capability polytope of a 3rrr planar parallel manipulator". In M. Ceccarelli and V.A. Glazunov, eds., *Advances on Theory and Practice of Robots and Manipulators*, Springer International Publishing, Vol. 22 of *Mechanisms and Machine Science*, pp. 537–545. ISBN 978-3-319-07057-5.

Mejia, L., Simas, H. and Martins, D., 2015. "Force capability in general 3dof planar mechanisms". *Mechanism and Machine Theory*, Vol. 91, No. 0, pp. 120 – 134.

Nokleby, S.B., Fisher, R., Podhorodeski, R.P. and Firmani, F., 2005. "Force capabilities of redundantly-actuated parallel manipulators". *Mechanism and Machine Theory*, Vol. 40, pp. 578–599.

Owen, W., Croft, E. and Benhabib, B., 2008. "Stiffness optimization for two-armed robotic sculpting". *Industrial robot: An International Journal, Vol. 35 Iss 1*, pp. 46–57.

Pan, Z., Zhang, H., Zhu, Z. and Wang, J., 2006. "Chatter analysis of robotic machining process". *Jornal of Materials Processing Technology*, Vol. 173, pp. 301–309.

Papadopoulos, E. and Gonthier, Y., 1995. "On manipulator posture planning for large force tasks". p. 6.

Siciliano, B., Sciavicco, L., Villani, L. and Oriolo, G., 2009. *Robotics: Modelling, Planning and Control*. London Limited, Springer-Verlag.

Stemmer, E.C., 1989. *Ferramentas de corte: ferramentas simples de tornear*. Ed. da UFSC, Florianópolis.

Subrin, K., Sabourin, L., Cousturier, R. and and, G.G., 2011. "Robotic drilling system for titanium structures". *Int. J. Adv. Manuf. Technol.*, Vol. 54, pp. 767–774.

Walker, I.D., Marcus, S.I. and Freeman, R.A., 1989. "Distribution of dynamic loads for multiple cooperating robot manipulators". *Journal of Robotic Systems*, Vol. 6, pp. 35–47.

Weihmann, L., Martins, D. and Coelho, L.S., 2011. "Force capabilities of kinematically redundant planar parallel manipulators". *13th World Congress in Mechanism and Machine Science*, p. 483.

Witte, L., 1980. *Spezifische Zerspankrä fte beim Drehen und Bohren*. Ph.D. thesis, RWTH, Aachen, Alemanha.

Zheng, Y.F. and Luh, J.Y.S., 1988. "Optimal load distribution for two industrial robots handling a single object". *IEEE International Conference on Robotics and Automation*, Vol. 1, pp. 344–349.

Zibil, A., Firmani, F., Nokleby, S. and Podhorodeski, R., 2007. "An explicit method for determining the force-moment capabilities of redundantly actuated planar parallel manipulators". *Journal of Mechanical Design, Transactions of the ASME*, Vol. 129, No. 10, pp. 1046–1055.

9. RESPONSIBILITY NOTICE

The authors are the only responsible for the printed material included in this paper.